Hindawi
International Journal of Antennas and Propagation
Volume 2019, Article ID 8023712, 9 pages
https://doi.org/10.1155/2019/8023712

Research Article

Planar Beam Steerable Parasitic Array Antenna System Design Based on the Yagi-Uda Design Method

Seok-Jae Lee[1,2] **Won-Sang Yoon**[3] **and Sang-Min Han**[1]

[1]*Department of Information and Communication Engineering, Soonchunhyang University, Asan, Chungnam 31538, Republic of Korea*
[2]*Key Technology R&D Institute, Wisol Inc., Gyeonggi 18103, Republic of Korea*
[3]*Division of Electronics and Display Engineering, Hoseo University, Asan, Chungnam 31499, Republic of Korea*

Correspondence should be addressed to Sang-Min Han; auspice0@gmail.com

Received 18 October 2018; Revised 21 February 2019; Accepted 7 March 2019; Published 2 May 2019

Academic Editor: Hervé Aubert

A planar beam steerable array antenna system is proposed with dual-control circuits for feeding and reactive loadings. Two orthogonally arranged planar dipoles are excited by SPDT switching circuits, while the forward and backward beam directions are controlled by the adjusted effective electric lengths of the parasitic dipole elements. The adjusted parasitic dipoles are designed to play the alternative roles of directors and reflectors based on the Yagi-Uda antenna theory. The proposed antenna system with four-way switchable beams has been implemented on a planar substrate and evaluated for orthogonal four-way beam steering performance with good agreement.

1. Introduction

Recent wireless communication services have been pursued with regard to high speed, real time, and massive connections. These requirements are focusing on the fifth-generation (5G) mobile standard including IoT connectivity services, which is expected to be commercially established in 2019 through the 3GPP LTE release 16 [1]. To increase communication efficiency, adaptive beamforming becomes an important issue in 5G technologies. The beamforming techniques have been developed toward compact and simple architectures such as conventional analog/hybrid/digital beamformings [2], retrodirective arrays [3], smart antennas [4, 5], reconfigurable patterns [6], and Electrically Steerable Parasitic Array Radiator (ESPAR) antennas [7–11]. The ESPAR antenna has switchable beams with orthogonal four directions. It consists of one active element antenna at the center and its surrounding parasitic element antennas with adjustable reactance loads for each beam direction. The parasitic element has been designed with various parasitic structures, such as monopoles [12], dipoles [13], and patch antennas [14]. However, due to the three-dimensional form factor, the conventional ESPAR antenna cannot be integrated with other planar circuits. Moreover, as it has only one parasitic element for each direction, its directivity and beamwidth are limited and uncontrollable. The additional parasitic element can increase the antenna gain and front-to-back (F/B) ratio.

In this paper, a new ESPAR antenna is designed with planar architecture based on the Yagi-Uda design methodology. Two parasitic elements are designed for each direction to take a higher directivity. The proposed antenna system can radiate four orthogonal beams by switching an excited active element and the roles of parasitic antenna elements from reflectors to directors and vice versa. The function of the parasitic element can be exchanged by adjusting the value of reactance mounted on each parasitic element. Therefore, the proposed planar beam steerable antenna is designed to operate with bidirectional beam control. Moreover, it has excellent capabilities to achieve a small form factor and to be integrable in planar subsystems. This paper is organized as follows. Following a brief introduction, the design and operation procedure of the proposed antenna system are described in Section 2. Section 3 explains the implementation

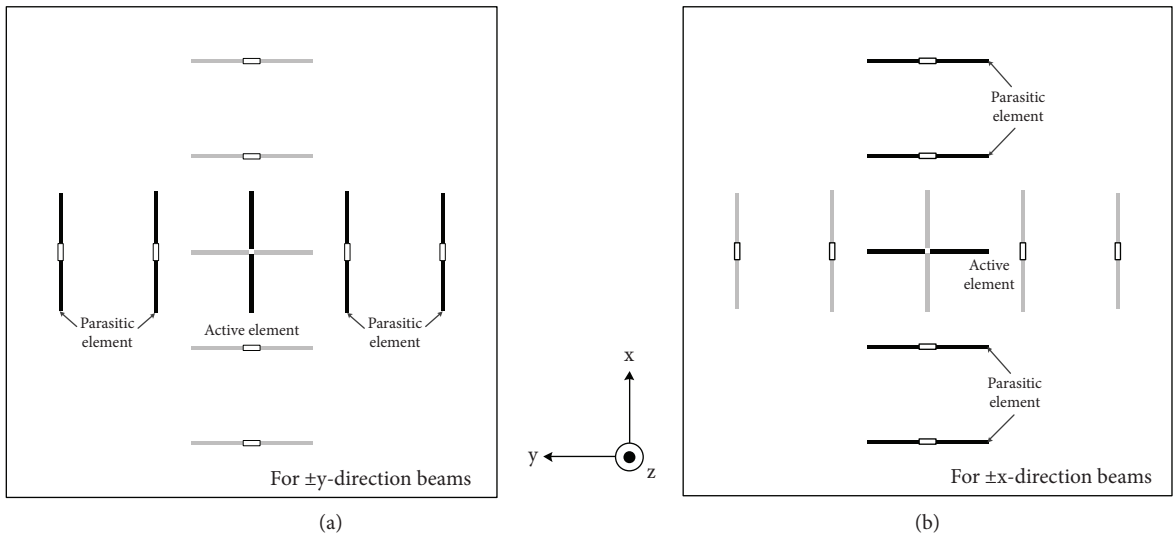

Figure 1: Orthogonal feeding process of the proposed planar beam steerable antenna.

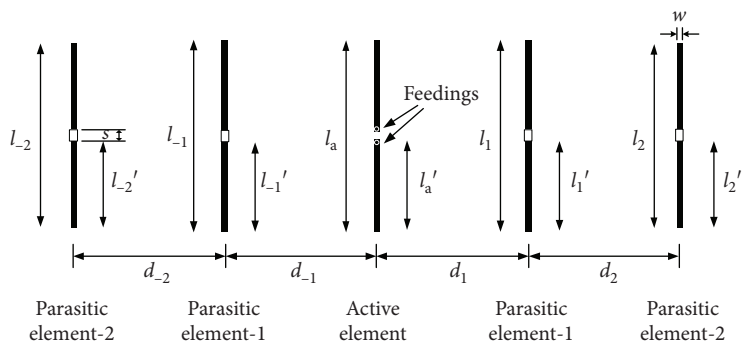

Figure 2: Linear switchable antenna array based on the Yagi-Uda array operation.

and the performance evaluation of the circuit and system. Finally, Section 4 provides the conclusion and discusses applications and commercial feasibility for the proposed system.

2. Planar ESPAR Antenna System Design

In this section, a planar ESPAR antenna system is designed with the Yagi-Uda array design method and its operating schemes are described. Figure 1 shows the top views of the proposed planar ESPAR antenna. It consists of two active element antennas with crossed dipole shapes and four two-stage parasitic element antennas parallel to each active dipole element. Figure 1(a) presents the operating status for the excitation to the y-directional beams, while the x-directional beams can be generated by solely feeding the horizontal active element as shown in Figure 1(b). As the excited active element antennas are cross-arranged with each other, the antenna system operates one by one. To shape the orthogonal beams, the two active dipoles require high isolation.

The Yagi-Uda array antenna was developed by Uda and Yagi in 1926 and 1928, respectively [15]. The Yagi-Uda antenna consists of several linear dipole elements. Whereas only one dipole is excited from an RF source called a driven element (active element), the other ones are called directors or reflectors (parasitic elements) in which microwave currents are induced by mutual coupling. As the Yagi-Uda antenna is designed to act as a longitudinal array [15–17], the parasitic elements located in a beam direction act as directors and those in the opposite side as reflectors. Since the quasi-Yagi antenna was introduced in [18], various planar architectures based on the Yagi-Uda theory have been developed with higher directivity and small form factor. A planar single quasi-Yagi antenna with V-shaped electronically controlled directors has shown to be a flexible antenna design due to the electronic control [19]. Furthermore, microstrip patch arrays based on the Yagi-Uda theory were researched with the antenna frequency and circular polarization switching [20, 21]. In this paper, a beam-switchable planar dipole array based on the Yagi-Uda methodology is presented.

Figure 2 describes the one-directional beam generation process based on the Yagi-Uda design method. The proposed antenna system controls the effective electric lengths of the parasitic elements to switch beam directions. As the number of parasitic elements determines the antenna directivity, two directors are utilized for a higher antenna directivity and F/B ratio, although the number of reflectors is normally not a significant factor. The excited active element at the center has

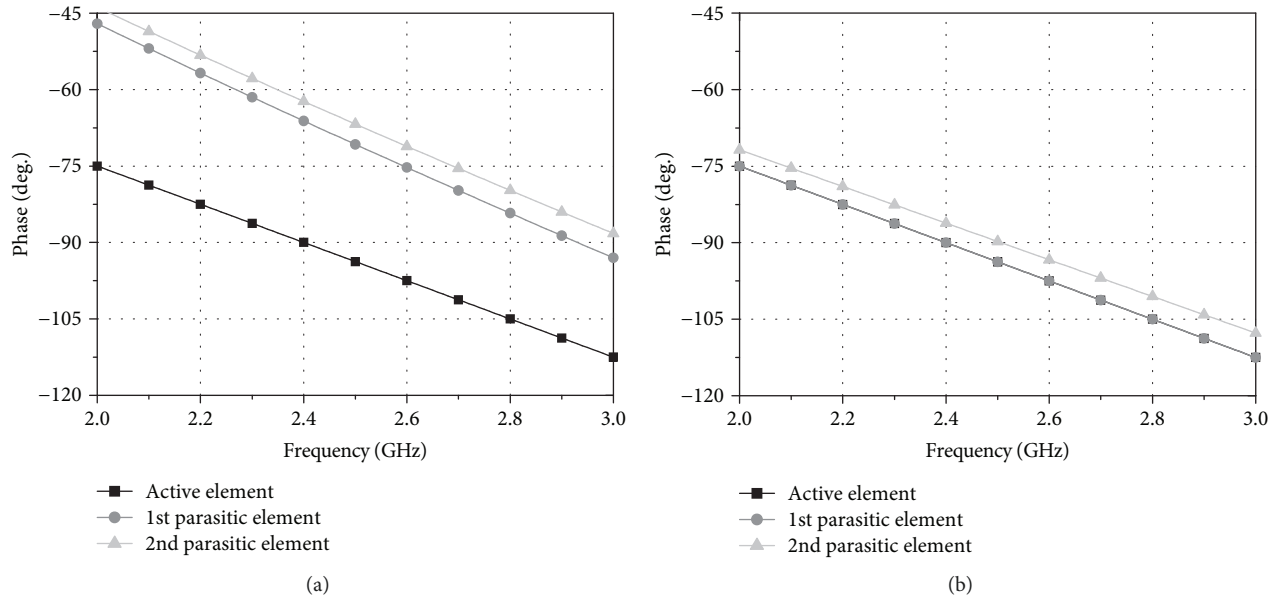

Figure 3: Effective electric lengths for parasitic elements relative to the $\lambda/2$ active element with a reactive load of (a) 1.5 pF for a director and (b) 0.1 μF for a reflector.

two parasitic elements for each bidirection. The electric length of the active element l_a is designed with about $\lambda_o/2$, whereas those of the parasitic elements l_{-2}, l_{-1}, l_1, and l_2 are optimized with adjustable reactance mounted between the feeding points. The separation between each element antenna of d_{-2}, d_{-1}, d_1, and d_2 is designed for directivity and impedance control at the range of $0.25\lambda_o$-$0.3\lambda_o$.

To switch the beam direction alternatively and to play the alternative roles of a director and a reflector, the lengths of the parasitic elements have to be changed. Therefore, the appropriate physical lengths of parasitic dipoles and the values of the reactance have to be found for a director and a reflector. Figure 3 presents ideal simulation results for the electric lengths of active and parasitic elements with reactive loads at 2.4 GHz. Each dipole is designed with an electric length of l_a, l_{-1}, and $l_1 = 90^\circ$ and l_{-2} and $l_2 = 86.2^\circ$. The reactance values connected to the centers of l_{-1} and l_{-2} are found at 1.5 pF for a director operation, and the others are 0.1 μF for a reflector operation. Figure 3(a) shows the different electric lengths of $l_a = 90^\circ$, $l_1 = 66.15^\circ$, and $l_2 = 62.31^\circ$ at 2.4 GHz for a director operation, while almost the same electric lengths of $l_a = 90^\circ$, $l_1 = 90^\circ$, and $l_2 = 86.16^\circ$ are presented for a reflector operation in Figure 3(b). Whereas the parasitic element mounted with a capacitance of 1.5 pF reduces the effective electric length, the one with a capacitance of 0.1 μF makes the stripline a short-circuited line. The forward-direction parasitic element (director) attains a relatively shorter electric length than the active element by mounting a capacitor of 1.5 pF. The backward-direction parasitic element (reflector) has almost the same electric length as the active element with large capacitance. From the specified reactance, the physical lengths of dipoles are optimized with an EM simulator (High Frequency Structure Simulator, ANSYS Ltd.) under the consideration of radiation beam patterns and impedance matching. The physical lengths of monopoles are $l'_a = 22.5$ mm, $l'_1 = 22.5$ mm, and $l'_2 = 21.5$ mm, the separation between each monopole is $s = 2$ mm, and the linewidths of all printed dipoles are $w = 1.5$ mm. The separation between element antennas is $d_x = 37$ mm.

From the theoretical design of the Yagi-Uda method, the full reconfigurable system is designed as shown in Figure 4, while the verification of the ideal antenna configuration with ideal reactive capacitances was presented in [10]. The switchable reactance is replaced with the impedance of the PIN diodes. The reactive diodes of D1-D8 are biased by rear-side bias lines through via holes that are displayed in gray lines. The bias voltage is supplied from 1.0 to 1.2 V for the port V1 to port V6. While the diode operates at an on status, the equivalent reactance is approximately 1.5 pF, which makes the parasitic element antenna operate as a director. For the off status of the diode, the parasitic element antenna becomes a reflector with a 0.1 μF reactance. Table 1 summarizes the proposed antenna system operation for supplied biases.

The feeding method for the active element antennas is described in Figure 5. To keep the balanced feeding of RF(+) and RF(-), two SPDT switches are utilized. Figure 5(a) shows the excitation to the vertically arranged active dipole by switching the feeding network, while Figure 5(b) describes the horizontally arranged active element. The two switched-output RF signals are fed from the rear side of the substrate.

3. Implementation and Experimental Results

In this section, the proposed planar beam steerable antenna system is implemented and evaluated for beam steering performance. The antenna system is fabricated on two FR4 substrates with a dielectric constant of 4.4 and a thickness of 1 mm for the antenna system and SPTD switching circuit boards. The antenna system board is implemented with a size

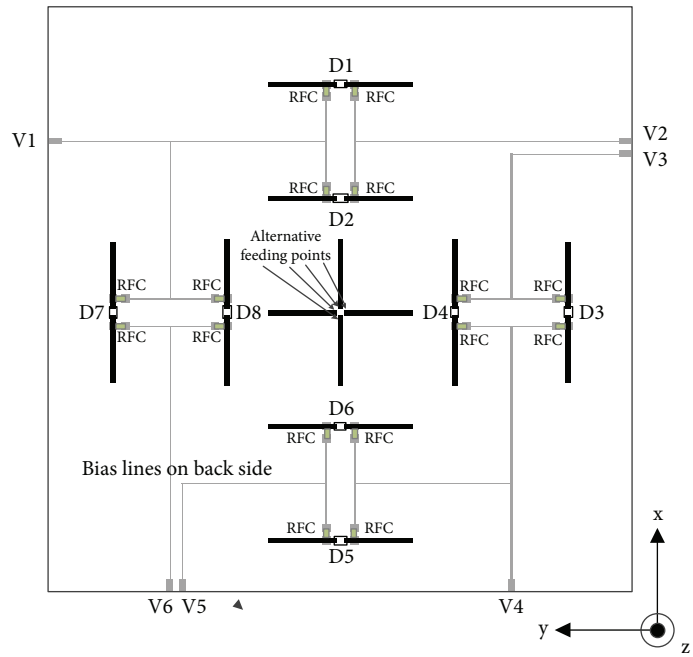

Figure 4: Configuration of the proposed planar ESPAR antenna system.

Table 1: Control voltages for diode status and beam directions.

Beam	V_1	V_2	V_3	V_4	V_5	V_6	D_1 & D_2	D_3 & D_4	D_5 & D_6	D_7 & D_8
$+x$	−	+	−	−	−	−	ON	OFF	OFF	OFF
$-x$	−	−	−	−	+	−	OFF	OFF	ON	OFF
$+y$	−	−	−	−	−	+	OFF	OFF	OFF	ON
$-y$	−	−	+	−	−	−	OFF	ON	OFF	OFF

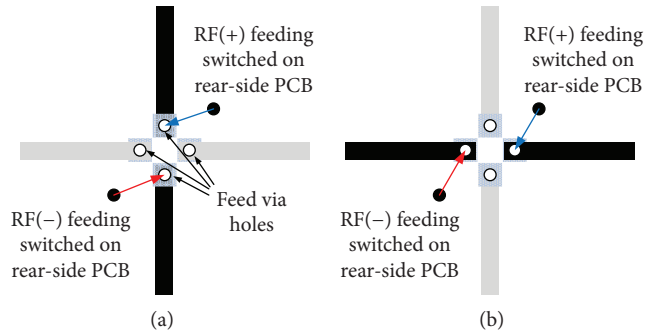

Figure 5: Switching excitations to the crossed active elements: (a) x-axis excitation; (b) y-axis excitation.

of $189.8 \times 189.8 \times 1.0$ mm^3, and each SPDT board has a dimension of $44.5 \times 37.57 \times 1.0$ mm^3.

3.1. Active Element Antennas. The active element antennas are fed through via holes from the rear side of the antenna board. The feedline is connected to the SPTD switching board. As the active dipole element antenna is fed with balanced signals, each RF(+) and RF(-) signal is provided. The HMC194MS8 CMOS diode (Hittite Microwave Corporation Ltd.) is controlled by switching voltages of V1 and V2 to switch the signal into the RF_{out1} or RF_{out2}. The selected RF signal is connected to the center feeding points of the active dipole antenna on the front side. Figure 6 presents the circuit layout of the SPDT switching board. The crossed dipole requires high isolation to generate orthogonal beam patterns and a relatively low crosspolarization level. The measured isolation presented high isolation of more than 35 dB.

To testify the orthogonal excitation to the active crossed dipoles without parasitic elements, the active element antenna operated with the switching feedlines is experimented on.

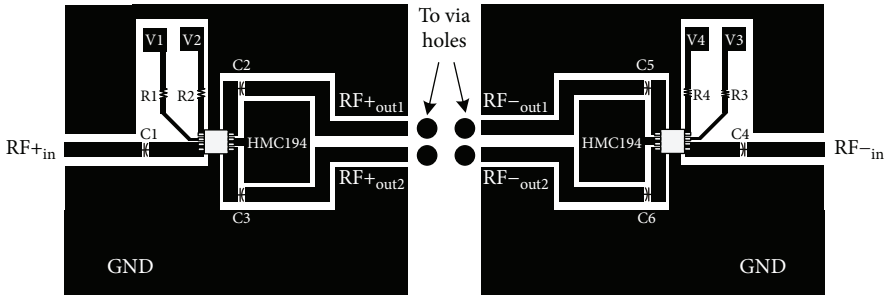

Figure 6: Layout of the SPDT switching circuit board using CMOS diodes for alternative feedings.

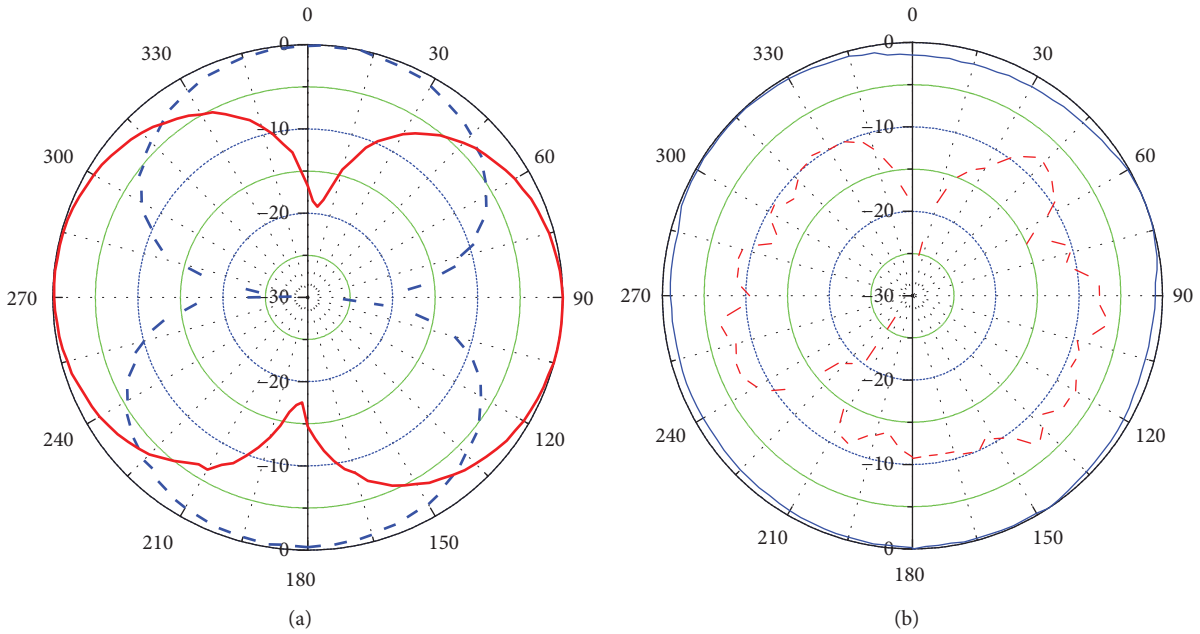

Figure 7: Radiation patterns of the active dipole antennas: (a) E-plane (solid line: y-axis excitation; dashed line: y-axis excitation); (b) H-plane (solid line: copolarization; dashed line: crosspolarization).

The measured return losses show more than 200 MHz bandwidth at 2.4 GHz. Almost the same matching characteristics are shown for both feeding schemes of x- and y-axis active elements. The radiation patterns are measured to investigate the switching performances. Figure 7(a) shows the measured E-plane radiation patterns for the y-axis excitation (solid line) and x-axis excitation (dashed line). The maximum gain shows 2.6 dBi. Figure 7(b) presents the measured H-plane radiation pattern with the crosspolarized pattern. The omnidirectional pattern is well generated with about a 10 dB crosspolarization level.

3.2. Parasitic Element Antennas. The parasitic element antenna is implemented with a reconfigurable reactance. The implemented layout for the parasitic element antenna is shown in Figure 8. The reactance is adjusted by a PIN diode (BAR 64-02V, Infineon Technologies Ltd.). It is biased from a rear-side bias circuit shown in gray color. The diode is mounted at the center of the dipole where the via hole is connected from back to front. To block the RF signal leakage, an RF choke is mounted between the via hole and a bias line.

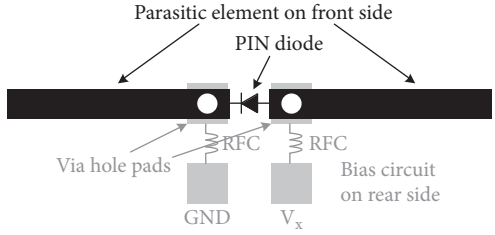

Figure 8: Layout of the parasitic element antenna mounting a reconfigurable reactive load with bias circuits.

When the bias voltage of about +1 V is provided, the reactive diode operates at a reactance of 1.5 pF and the parasitic element antenna plays the role of a director. While the diode is off, it has a large capacitance of 0.1 μF for a reflector. Because the PIN diode mounted between planar monopoles does not operate on a microstrip environment without a ground plane, the deembedded calibration method is used for the extraction [22]. The forward resistance of PIN diodes results in antenna gain degradation.

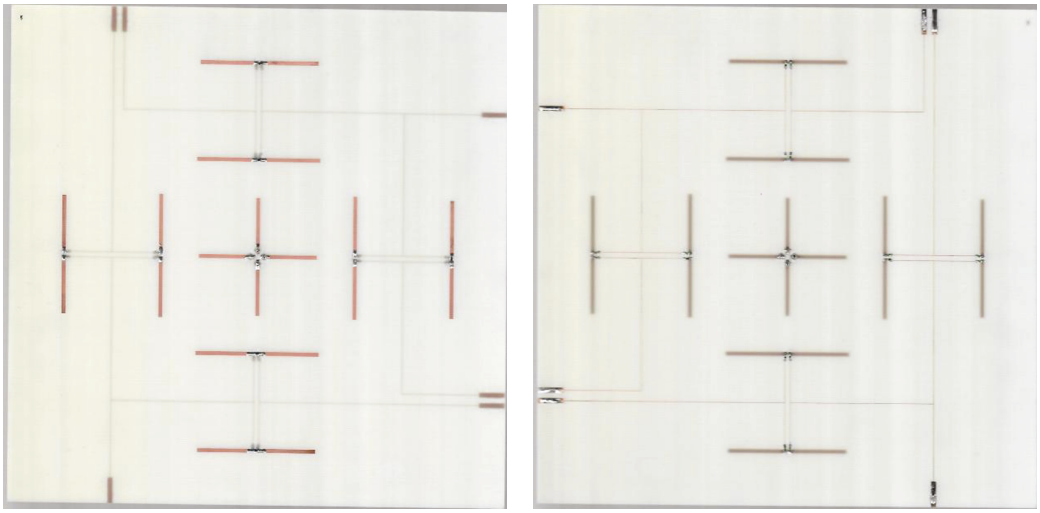

(a) Front view (b) Rear view

Figure 9: Photographs of the beam steering antenna system.

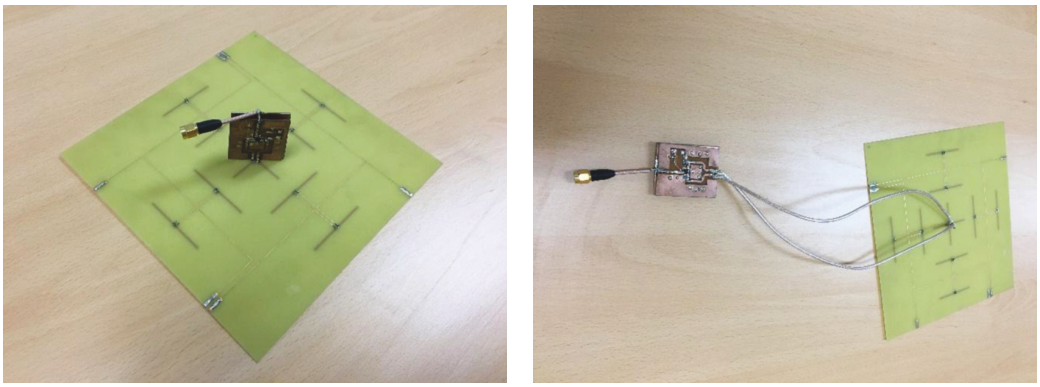

(a) Direct connection (b) Cable connection

Figure 10: Photographs of the integrated beam steering system with two alternative assembly techniques.

3.3. Integration of the Proposed Antenna System. The planar beam steerable antenna and SPDT switching circuit boards are implemented and integrated to evaluate the reconfigurable beam radiations. Figure9(a) shows a photograph of the front-side view with only active elements and parasitic dipole elements mounting PIN diodes that contribute to main beam radiation. The rear side has bias lines and RF chokes behind the dielectric substrate to reduce perturbation of unwanted radiation as shown in Figure 9(b). Due to the transparency of FR4 epoxy, the backside metallic patterns reflect each other in the photographs.

The two system parts of the planar antenna and SPDT boards are integrated. Two assembly techniques can be applied for efficient system operation. First, the SPDT boards with ground planes facing each other are directly connected to the feeding points of the planar antenna board. To avoid the metallic effect on active elements, the SPDT boards are perpendicularly connected with a 45° oblique angle as shown in Figure 10(a). This assembly can minimize insertion loss and prevent phase mismatching. Alternatively, the antenna board can be connected to

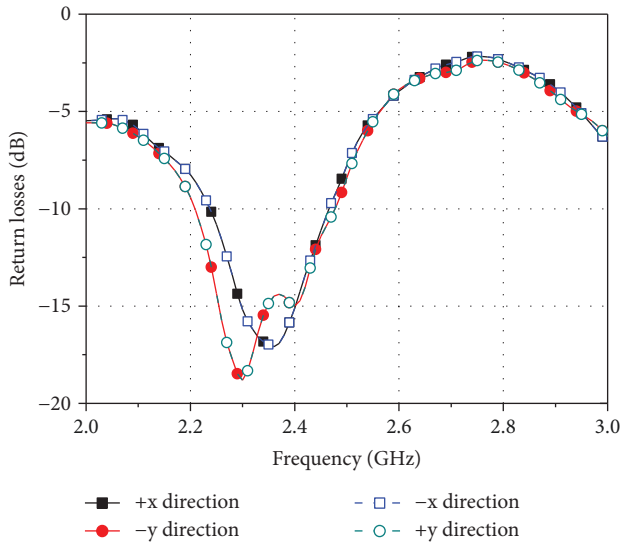

Figure 11: Return losses of the proposed antenna system for each beam direction.

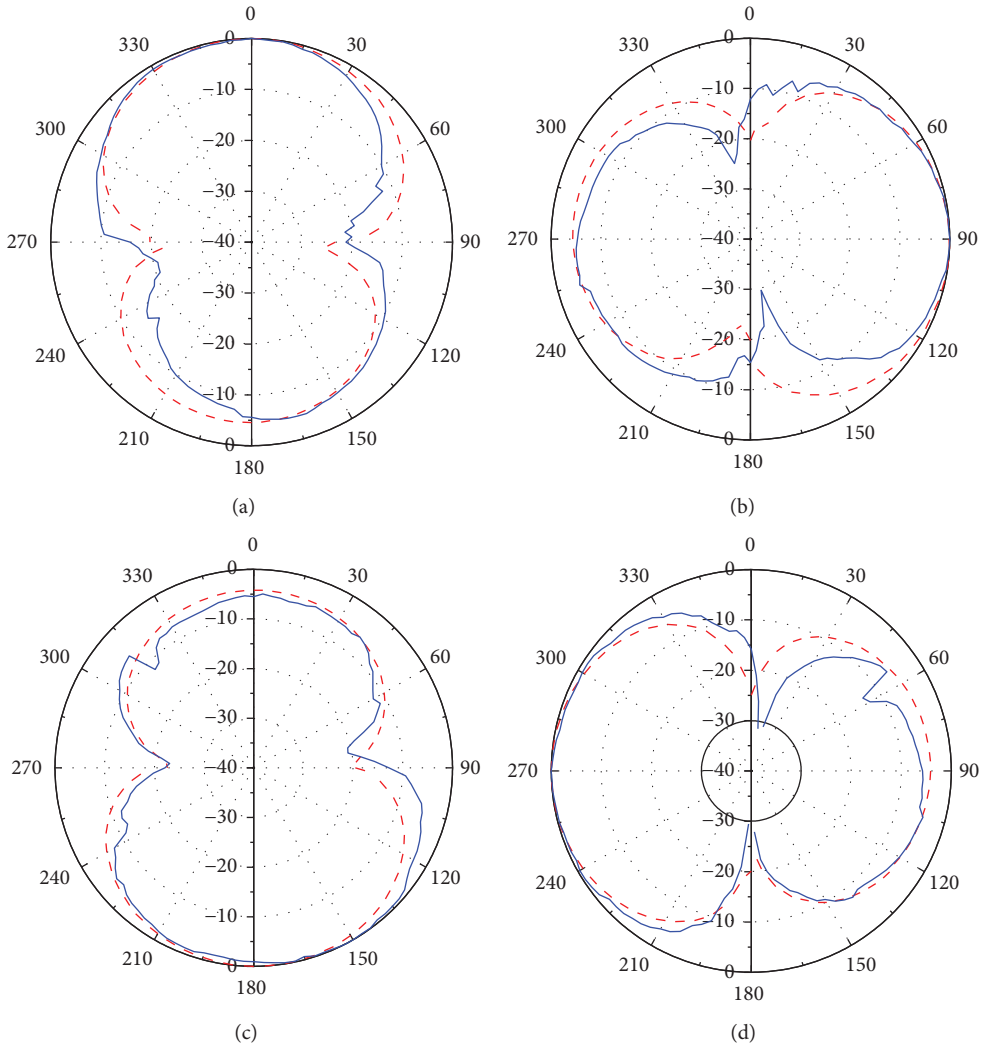

Figure 12: Beam steered radiation patterns for each direction with the reactive loads of a diode (solid line) and a chip capacitor (dashed lines): (a) +y-direction; (b) +x-direction; (c) -y-direction; (d) +x-direction.

the SPDT through two equal length coaxial cables as shown in Figure 10(b). It can reduce radiation perturbation but increases loss and phase unbalance. Both methods can be chosen for the system integration with the other modules and subsystems. The former method was adopted for the measurements in Section 4.

3.4. Performance Evaluation of the Proposed Planar Beam Steerable Antenna System. The proposed planar beam steerable antenna system is experimentally evaluated in this section. Figure 11 presents the return losses for four beamforming setups. The return losses show almost the same characteristics with impedance bandwidths of 230–270 MHz at a reference of 10 dB return loss. Due to the switching excitation, the x-direction and y-direction characteristics have slightly different results.

The switching radiation beams are experimented on with two types of reactive loads to compare with ideal results. Ideal chip capacitors and electrically controlled reactive diodes are mounted and measured, respectively. Chip capacitors of 1.5 pF are mounted for the parasitic element antennas located in the beam direction, and 0.1 μF capacitors are used for the other ones. The measured radiation patterns are presented in Figure 12. The solid lines show the full electrically reconfigured beam patterns, and the dashed lines present beam patterns by ideal chip capacitors. The experimental results show the four-way switchable directional radiation patterns. Each beam is well directed to specified orthogonal ways. It presents a maximum antenna gain of 5.9 dBi with a 1 dB power gain bandwidth of 65 MHz and a 3 dB power gain bandwidth of 140 MHz. And its radiation pattern has 1 dB beamwidths of 50–60° and 3 dB half-power beamwidths of 90–93°. Compared with the ideal passive antenna gain in [10] of 10.7 dB, about 4.8 dB of gain degradation is caused by the forward resistance of PIN diodes and bias circuits.

To evaluate antenna system performance, the system link budget is analyzed from the single feeding point to effective isotropic radiation power (EIRP) as shown in Table 2. The IEEE 802.11b specification is applied for a 2.4 GHz ISM band [23]. Maximum transmitting power is set to 33 dBm, and a

Table 2: Link budget analysis for the IEEE 802.11b specification.

	Single feeding	SPDT	Antenna	EIRP
Gain/loss (dB)		-4.7	5.9	
P_tx (dBm)	33	28.3		34.2
P_rx (dBm)	-76	-80.7		-74.8

minimum sensitivity level of -76 dBm at an antenna feeding point is applied.

4. Conclusions

In this paper, a planar beam steerable antenna system was proposed. The proposed antenna was designed using the Yagi-Uda array design methodology on a planar substrate with bidirectional beam-switching characteristics. Two orthogonally arranged arrays operated the bidirectional beam switching by adjusting the reactance of the parasitic elements. The design method using the Yagi-Uda theory and electrical antenna length variation was presented. From the experimental results, the proposed antenna system was verified for the beam steering ability to the orthogonal four directions. As the proposed antenna system could be implemented on a single fabrication process with other PCB components on a planar substrate, it would be an excellent candidate for small form factor beam steering antenna system applications.

Data Availability

The graph and table data used to support the findings of this study are included within the article.

Conflicts of Interest

The authors declare that they have no conflicts of interest.

Acknowledgments

This research was supported by the Ministry of Science and ICT, Korea, under the ITRC support program supervised by the IITP and the Soonchunhyang University research fund (IITP-2019-0-00403).

References

[1] M. Shafi, A. F. Molisch, P. J. Smith et al., "5G: a tutorial overview of standards, trials, challenges, deployment, and practice," *IEEE Journal on Selected Areas in Communications*, vol. 35, no. 6, pp. 1201–1221, 2017.

[2] V. Venkateswaran, F. Pivit, and L. Guan, "Hybrid RF and digital beamformer for cellular networks: algorithms, microwave architectures, and measurements," *IEEE Transactions on Microwave Theory and Techniques*, vol. 64, no. 7, pp. 2226–2243, 2016.

[3] R. Y. Miyamoto and T. Itoh, "Retrodirective arrays for wireless communications," *IEEE Microwave Magazine*, vol. 3, no. 1, pp. 71–79, 2002.

[4] A. Alexiou and M. Haardt, "Smart antenna technologies for future wireless systems: trends and challenges," *IEEE Communications Magazine*, vol. 42, no. 9, pp. 90–97, 2004.

[5] M.-S. Lee, J.-Y. Park, V. Katkovnik, T. Itoh, and Y.-H. Kim, "Adaptive robust DOA estimation for a 60-GHz antenna-array system," *IEEE Transactions on Vehicular Technology*, vol. 56, no. 5, pp. 3231–3237, 2007.

[6] W.-S. Yoon, J.-W. Baik, H.-S. Lee, S. Pyo, S.-M. Han, and Y.-S. Kim, "A reconfigurable circularly polarized microstrip antenna with a slotted ground plane," *IEEE Antennas and Wireless Propagation Letters*, vol. 9, pp. 1161–1164, 2010.

[7] A. Kalis, A. G. Kanatas, and C. B. Paradias, *Parasitic Antenna Arrays for Wireless MIMO Systems*, Springer, New York, NY, USA, 2014.

[8] N. Honma, K. Nishimori, R. Kudo, Y. Takatori, T. Hiraguri, and M. Mizoguchi, "A stochastic approach to design MIMO antenna with parasitic elements based on propagation characteristics," *IEICE Transactions on Communications*, vol. E93-B, no. 10, pp. 2578–2585, 2010.

[9] A. Kalis, C. Papadias, and A. G. Kanatas, "An ESPAR antenna for beamspace-MIMO systems using PSK modulation schemes," in *2007 IEEE International Conference on Communications*, pp. 5348–5353, Glasgow, UK, 2007.

[10] S.-J. Lee, W.-S. Yoon, and S.-M. Han, "Planar directional beam antenna design for beam switching system applications," *Journal of Electromagnetic Engineering and Science*, vol. 17, no. 1, pp. 14–19, 2017.

[11] K. Ito, A. Akiyama, and M. Ando, "Bandwidth of electronically steerable parasitic array radiator antennas in single beam scanning," *IEICE Transactions on Communications*, vol. E86-B, no. 9, pp. 2844–2847, 2003.

[12] E. Taillefer, A. Hirata, and T. Ohira, "Direction-of-arrival estimation using radiation power pattern with an ESPAR antenna," *IEEE Transactions on Antennas and Propagation*, vol. 53, no. 2, pp. 678–684, 2005.

[13] N. Sakai, H. Uehara, and T. Ohira, "Variable beamforming characterization of a 3-element dipole ESPAR antenna from a complexity-of-directivity viewpoint," in *2009 Asia Pacific Microwave Conference*, pp. 751–754, Singapore, 2009.

[14] S. H. Yeung, A. Garcia-Lamperez, T. K. Sarkar, and M. Salazar-Palma, "Thin and compact dual-band four-element broadside patch antenna arrays," *IEEE Antennas and Wireless Propagation Letters*, vol. 13, pp. 567–570, 2014.

[15] H. Yagi, "Beam transmission of ultra short waves," *Proceedings of the IRE*, vol. 16, no. 6, pp. 715–740, 1928.

[16] R. Mailloux, "Antenna and wave theories of infinite Yagi-Uda arrays," *IEEE Transactions on Antennas and Propagation*, vol. 13, no. 4, pp. 499–506, 1965.

[17] R. Schlub and D. V. Thiel, "Switched parasitic antenna on a finite ground plane with conductive sleeve," *IEEE Transactions on Antennas and Propagation*, vol. 52, no. 5, pp. 1343–1347, 2004.

[18] Y. Qian, W. R. Deal, N. Kaneda, and T. Itoh, "Microstrip-fed quasi-Yagi antenna with broadband characteristics," *Electronics Letters*, vol. 34, no. 23, p. 2194, 1998.

[19] P.-Y. Qin, Y. J. Guo, and C. Ding, "A beam switching quasi-Yagi dipole antenna," *IEEE Transactions on Antennas and Propagation*, vol. 61, no. 10, pp. 4891–4899, 2013.

[20] D. Gray, J. W. Lu, and D. V. Thiel, "Electronically steerable Yagi-Uda microstrip patch antenna array," *IEEE Transactions on Antennas and Propagation*, vol. 46, no. 5, pp. 605–608, 1998.

[21] N. Honma, T. Seki, K. Nishikawa, K. Tsunekawa, and K. Sawaya, "Compact six-sector antenna employing three intersecting dual-beam microstrip Yagi–Uda arrays with common director," *IEEE Transactions on Antennas and Propagation*, vol. 54, no. 11, pp. 3055–3062, 2006.

[22] S.-M. Han, J. Lim, D. Ahn, and W.-S. Yoon, "A study of active element characterization by de-embedded calibration measurements," in *Proceedings of URSI General Assembly & Scientific Symposium (GASS)*, Montreal, Canada, 2017.

[23] Keysight Technologies, *IEEE 802.11 Wireless LAN PHY Layer (RF) Operation and Measurement – Application Note*, Keysight Technologies, 2017.